X95-11005

# DAMAGE TOLERANCE BASED LIFE PREDICTION METHODOLOGY IN CERAMIC MATRIX COMPOSITES

LOUIS J. GHOSN*
Case Western Reserve University
Cleveland, Ohio

and
Dennis W. Worthem**
Nyma, Inc.
Lewis Research Center Group
Brook Park, Ohio

## Introduction

Ceramic matrix composites (CMCs) are candidate materials for high temperature aerospace applications where high strength and low weight requirements are essential for more efficient engines. One advantage of continuous fiber reinforced ceramics over monolithic ceramics is an increase in fracture toughness due to the presence of bridging fibers in the crack wake which reduces the crack driving force. Before these ceramic matrix composite materials can be widely used in actual engine applications, life prediction methodologies have to be established based on the observed failure mechanisms.

Extensive experimental studies of various CMCs have shown that cracks propagate in the ceramic matrix, while leaving unbroken fibers to bridge the crack surfaces (refs. 1 to 3). The unbroken fibers in the wake of the crack restrict the opening of the matrix cracks and serve to shield the crack tip and reduce the crack driving force. However, these bridging fibers and interfaces are also vulnerable to harsh oxidative attacks, creep deformation, and excessive wear under fatigue conditions, which result in a progressive failure of these fibers and lead to accelerated crack growth and catastrophic failure. This delayed fiber failure has been shown to be associated with fretting and wear along the debonded interfaces of the bridging fibers, which occurs either during cyclic loading or long term exposure to high temperature (ref. 1 and 5).

Experimental studies have also shown the development of a periodic array of matrix cracks in both unidirectional glass ceramic systems (SiC/LAS ref. 3) and 2-D woven (SiC/SiC ref. 1) CMCs. The average crack spacing normalized to the specimen width is 0.35 for the 2-D SiC/SiC composite system, (Fig. 2). In the 2D woven SiC/SiC system, the measured crack periodicity is associated with the woven architecture. In that system, the periodic matrix cracks are observed in the inter-bundles matrix-rich regions adjacent to the free edges. These cracks ultimately arrest at the 0° bundles. This measured spacing of h/W=0.35 is postulated to influence the crack tip stress intensity factor and thus the crack driving force. Consequently, the objective of this presentation is to investigate the effects of periodic arrays of bridged cracks for various crack spacing ranging from h/W=0.2 to h/W=1.0 on the crack driving force. The effect of bridging is analyzed using the shear lag model developed by Marshall, Cox and Evans (Ref. 3). In their formulation, the effect of the bridging fibers is modelled as a nonlinear closure pressure proportional to the square root of the crack opening displacement. The proportionality constant, B (henceforth called bridging constant) is related to the square root of the interfacial frictional shear stress, $\tau$, as well as volume fraction, fiber radius and moduli of the matrix, fiber and composite.

---

* NASA Resident Research Associate at Lewis Research Center, under Grant NCC3-331.
** Work done under NASA Contract NAS3-25266.

## Analysis

The finite element analysis was used to determine the effective stress intensity factor for a periodic array of bridged edge cracks. The closure pressure was implemented as a nonlinear spring foundation in the bridge zone. Figure 4 shows the sub-model boundary conditions. A plane strain 2-dimensional model is assumed. Initially, the stress intensity factor of an array of unbridged multiple edge cracks is determined under constant global displacement as well as a point load along the crack wake at a distance $x_p$ from the free edge. Finally the shear lag model (ref. 4) is incorporated in the finite element analysis.

## Results

The normalized stress intensity factors (SIFs) for unbridged multiple edge cracks are shown in Fig. 5 as a function of normalized crack length ranging between 0.2 to 1.0 for a uniform global displacement. For small crack length (a/W>0.05) the effect of crack spacing is small. As the crack length increases, the SIF decreases and reaches a minimum before increasing. This decrease in the SIF is an added shielding mechanism that improves the durability of these materials. The ultimate increase in the SIF after reaching a minimum value is associated with the interaction of the collinear cracks along the same plane. The SIF decreases as the crack spacing decreases. The minimum value locations are in the range of a/W between 0.35 and 0.55 for h/W between 0.2 and 1.0.

The evaluation of the effect of crack spacing on the SIF for a periodic array of edge cracks is shown in Fig. 6 for various point loads along the crack wake for one crack length a/W=0.5. This solution is useful in formulating the closure pressure for a periodic array of bridged edge cracks. As the crack spacing increases, the SIF increases in a similar manner to the uniform global displacement solutions. However, in this case, as the point load moves closer to the crack tip, the stress intensity factor continuously increases.

The effects of crack spacing on bridging cracks are shown in Figs. 8 through 11. The variation of periodic bridged cracks with crack length is shown in Fig. 8 for two h/W (0.35 & 1.0). As the crack advances in the bridging zone, the SIF decreases before reaching a steady state value at a/W>0.8. The steady state SIF value is a function of crack spacing. The steady state SIF increases with increasing crack spacing.

The variation of the SIF with interfacial frictional shear stress is shown in Fig. 9. The normalized stress intensity factor is plotted as a function of the bridging constant, B, which is proportional to $\sqrt{\tau}$. The sensitivity of the SIF with crack spacing decreases as $\tau$ increases. For deep bridged cracks (a/W>0.5) with high interfacial shear stress, the dominant shielding mechanism is the bridging mechanism, and the effect of crack spacing is minimal. However, if $\tau$ increases, the bridging fiber stresses (C(x) in Fig. 7) also increase. This increase in fiber stresses will be detrimental when the bridging fibers start failing. Therefore, the interfacial shear stress should be tailored to maximize crack tip shielding from both crack spacing and fiber bridging without fiber failure.

The crack mouth opening displacement (CMOD) and effective crack modulus are plotted as a function of the bridging constant B in Figs. 10 and 11, respectively, for h/W=0.35 and 1.0. As h/W and the bridging constant B ($\alpha\sqrt{\tau}$) decrease, the CMOD decreases. Furthermore, for the same h/W, the CMOD increases with increasing crack length. However, this increase in CMOD with crack length decreases with increasing B, making the monitoring of crack extension more laborious for high interfacial frictional shear stresses. Similar observations can be deduced from the variation of the composite effective modulus with $\tau$ (see Fig. 11). The variation of the effective modulus with crack length decreases with increasing $\tau$. Furthermore, as h/W and $\tau$ increase, the effective modulus approaches the uncracked composite modulus.

The effect of fiber degradation is modelled as a reduction in stiffness of the bridging fibers. Hence, the fiber modulus in the shear lag bridging constant, B, is assumed to be a function of time, stress and temperature. The effective fiber degradation relationship is established from creep data of SiC fibers generated by Morscher & DiCarlo (ref. 5), see Fig. 12. The calculated SIF as a function of time is shown in Fig. 13, assuming an

instantaneous loading up to 130MPa before holding the displacement constant. The load in the composite decreases with time. The variation in average stress for various crack length and crack spacing is not noticeable. However, the SIF increases with time for various crack lengths, a/W, and crack spacings, h/W. In the present analysis, the time dependent degradation was limited to the fiber modulus. However, other parameter such as the interfacial shear stress and fiber strength can also be degraded in a similar manner once a functional relation is determined.

Finally, in a 2-D woven composite system, the 90° bundles do not contribute to fiber bridging. Thus, matrix cracks will transverse the 90° bundles region with no bridging. Figure 14 shows the variation of the SIF with crack length for both a continuous and discontinuous bridging zone. Also shown is the variation of the SIF for a continuous unbridged crack. As the crack reaches a 90° bundle, the SIF starts to increase due to the reduction in closure pressure in the crack wake. However, as soon as the crack reaches a 0° bundle, the SIF starts to decrease again toward the continuously bridged solution.

## Conclusions

The crack spacing observed in a SiC/SiC 2-D weave plays a role in shielding the crack tip, thus reducing the stress intensity factor. However, for periodic arrays of bridged cracks, the influence of crack spacing is a function of the interfacial shear strength and consequently the bridging constant. If the interfacial friction shear stress is too high, the effect of crack spacing diminishes. Thus shorter crack spacings can develop in ceramic composite systems with high interfacial frictional shear strength. Finally, the interfacial frictional shear stress ought to be optimized to take advantage of the shielding effect of the crack spacing mechanism as well as the fiber bridging mechanism.

## References


1. Worthem, D.W., Thermomechanical Fatigue Behavior of Coated and Uncoated Enhanced SiC/SiC[PW]. Hitemp Review 1994: Advanced High Temperature Engine Materials Technology Program, vol. III, NASA CP 10146, 1994, pp. 66-1, 66-12.

2. Chulya, A. and Brewer, A.R., A Study of Fiber Bridging Mechanisms in Ceramic Composites Via Crack Opening Displacement. Hitemp Review 1993: Advanced High Temperature Engine Materials Technology Program, vol. I, NASA CP 10081, 1993, pp. 24-1, 24-11.

3. Marshall, D.B., Cox, B.N., and Evans, A.G., The Mechanics of Matrix Cracking in Brittle-Matrix Fiber Composites. Acta Metallurgical, vol. 33, 1985, pp. 865-879

4. McMeeking, R.M., and Evans, A.G., Matrix Fatigue Cracking in Fiber Composites. Mechanics of Materials, vol. 9, 1990, pp. 217-227.

5. Morscher, G.N., and DiCarlo, J.A., Creep and Stress Relaxation of SiC-Based and $Al_2O_3$-Based Polycrystalline Fibers. Hitemp Review 1991: Advanced High Temperature Engine Materials Technology Program, NASA CP 10082, 1991, pp. 78-1, 78-13.

# OBJECTIVES

- **Determine the stress intensity factor for multiple cracks in a ceramic matrix composite system as a function of crack length and crack spacing.**

- **Incorporate the Shear Lag model to simulate the effects of bridging fibers in a multi-cracked body.**

Fig. 1

# MOTIVATION

**Multiple cracking observed in fatigued CMCs' smooth specimens**

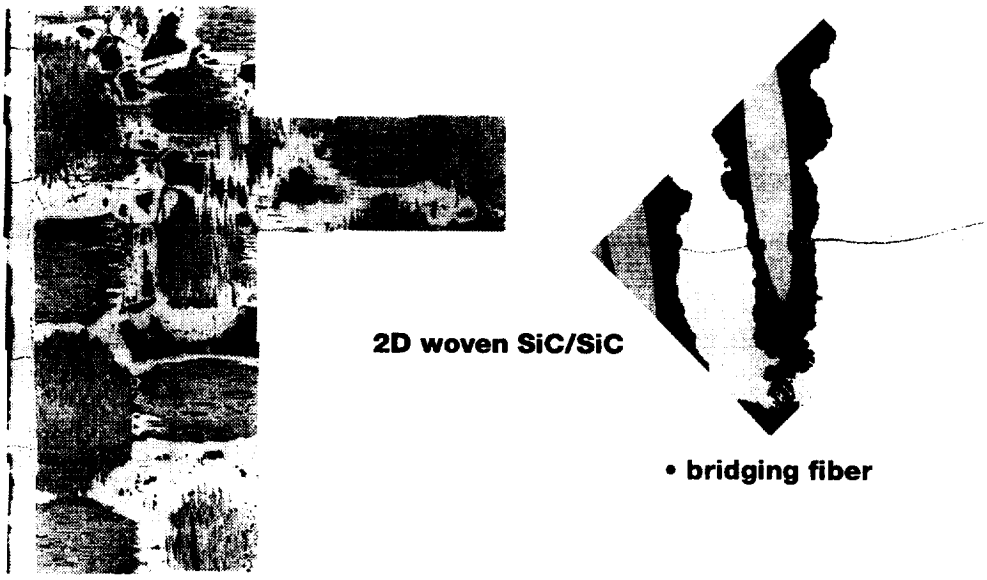


**average crack spacing h/W = 0.35**

Fig. 2

# IDEALIZATION OF A MULTI-CRACKED CMC

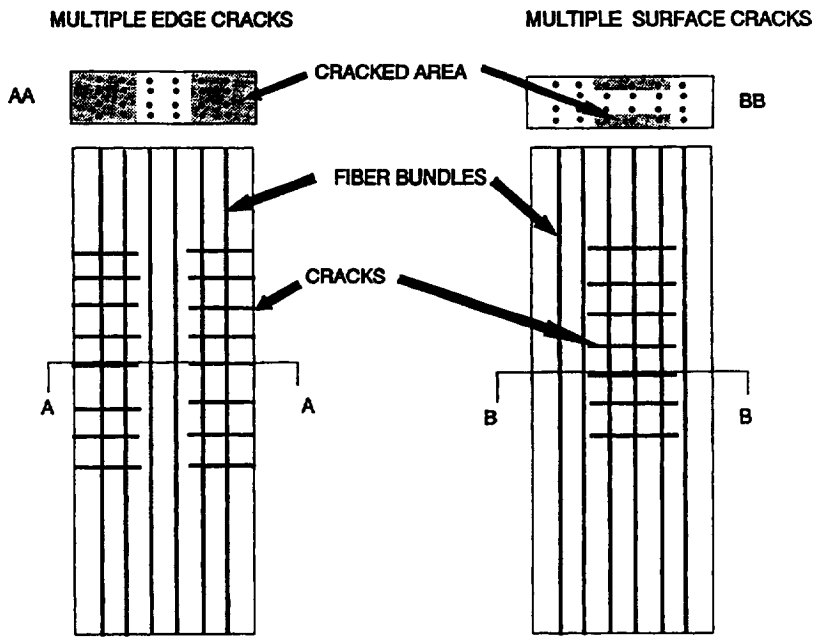


Fig. 3

# ANALYTICAL SOLUTION

## finite element method applied to a sub-region

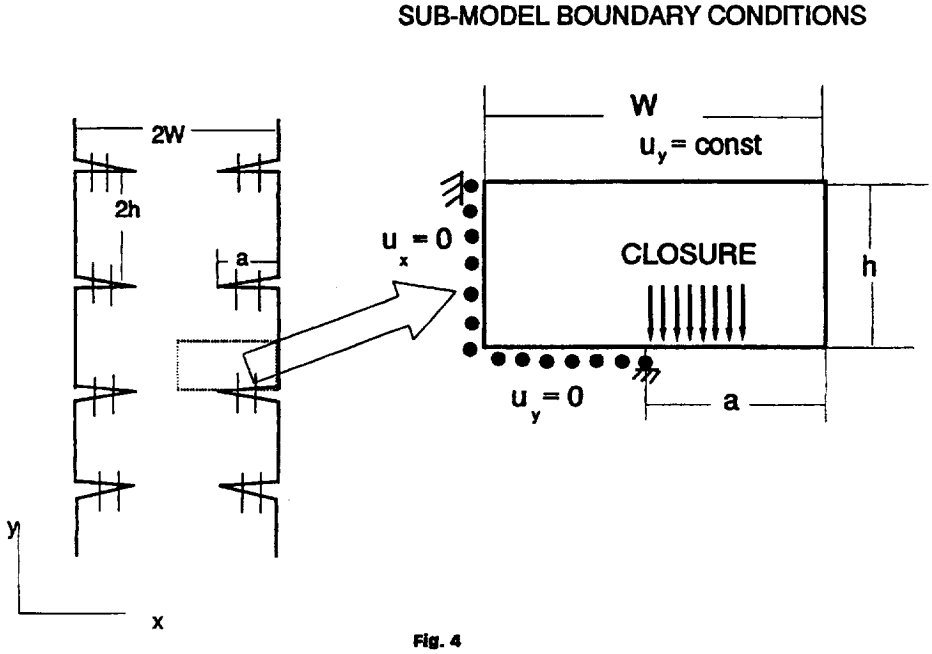


Fig. 4

# NORMALIZED STRESS INTENSITY FACTOR FOR MULTIPLE DOUBLE EDGE NOTCH SPECIMENS

## uniform remote load with no bridging

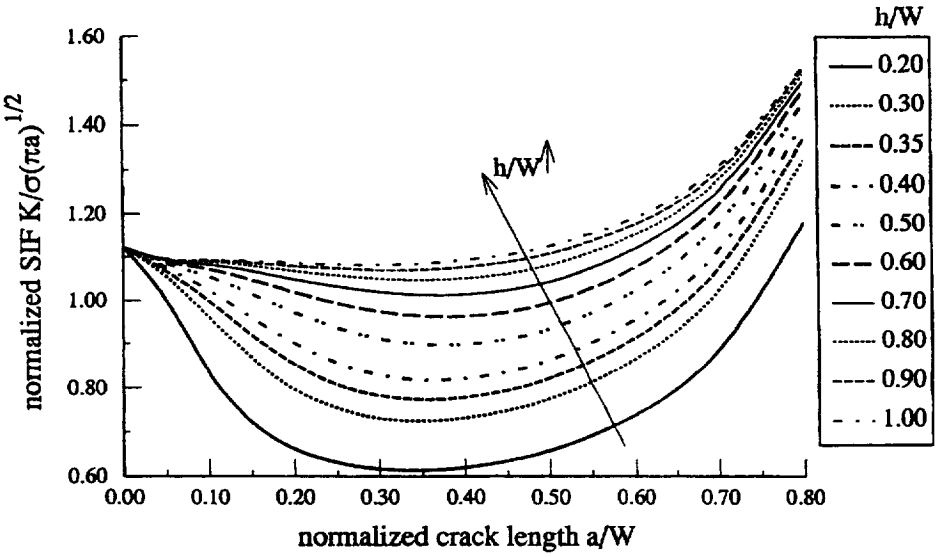


- **stress intensity factor (SIF) decreases as the crack spacing decreases**

Fig. 5

# NORMALIZED STRESS INTENSITY FACTOR FOR MULTIPLE DOUBLE EDGE NOTCH SPECIMENS

## point load along the crack faces for a/W = 0.5

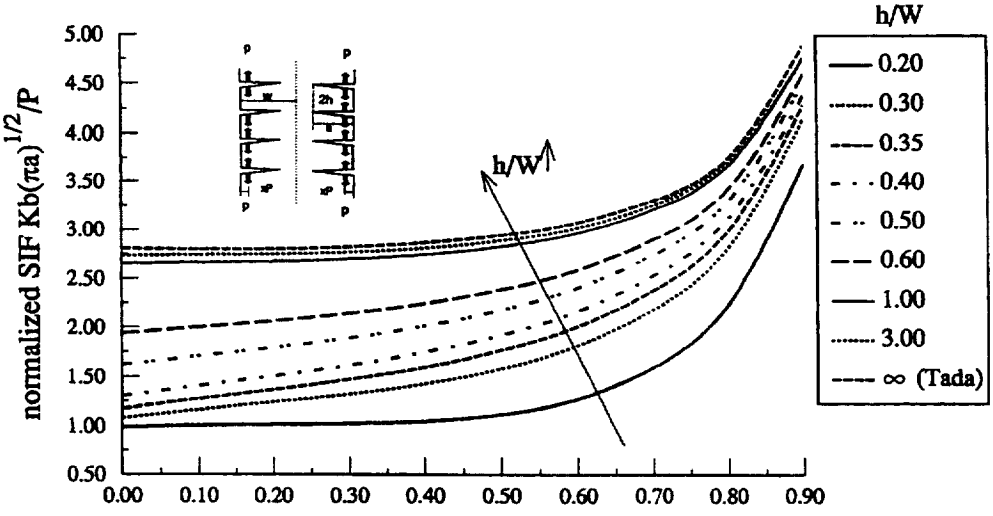


- **SIF decreases with a decrease in crack spacing**

Fig. 6

# SHEAR-LAG MODEL FOR FIBER BRIDGING

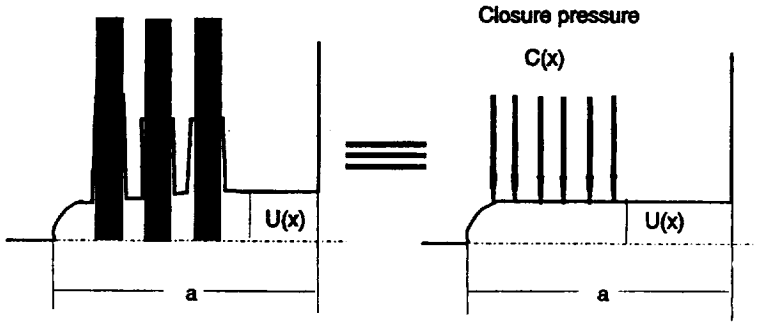


$$\textit{Monotonic:}\quad C(x) = 2\sqrt{\frac{U(x)\,\tau\,V_f^2 E_f E_c^2}{R(1-V_f)^2 E_m^2}}$$

$$C(x) = B\sqrt{U(x)}$$

$$\textit{Fatigue:}\quad \Delta C(x) = 2\sqrt{\frac{2\Delta U(x)\,\tau\,V_f^2 E_f E_c^2}{R(1-V_f)^2 E_m^2}}$$

**bridging constant B** $\propto \sqrt{\tau}$

**(reference McMeeking and Evans)**

**Fig. 7**

# SIF VARIATION WITH FIBER BRIDGING

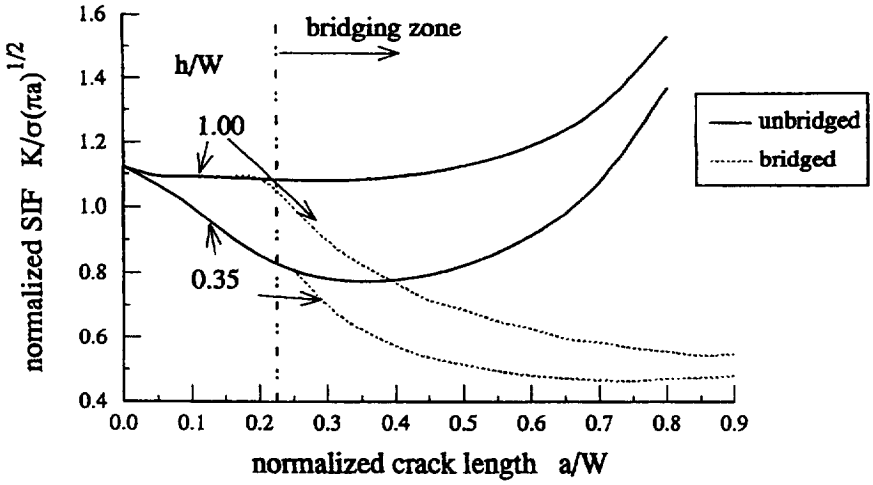


- **the effect of crack spacing is evidence even when bridging is applied**

**Fig. 8**

# VARIATION OF THE SIF FOR MULTI-CRACKED BODY

as a function of
- bridging constant, B $\propto \sqrt{\tau}$
- crack length, a/W
- crack spacing, h/W

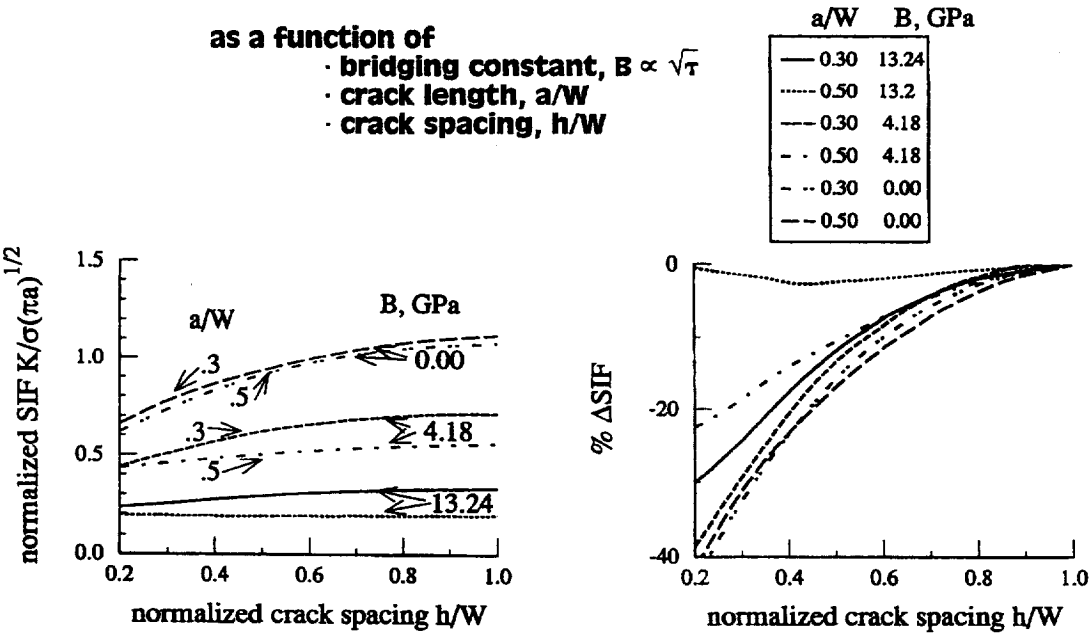


- as $\tau$ increases the variation in SIF with spacing decreases

Fig. 9

# VARIATION OF CRACK OPENING DISPLACEMENT WITH THE BRIDGING CONSTANT B $\propto \sqrt{\tau}$

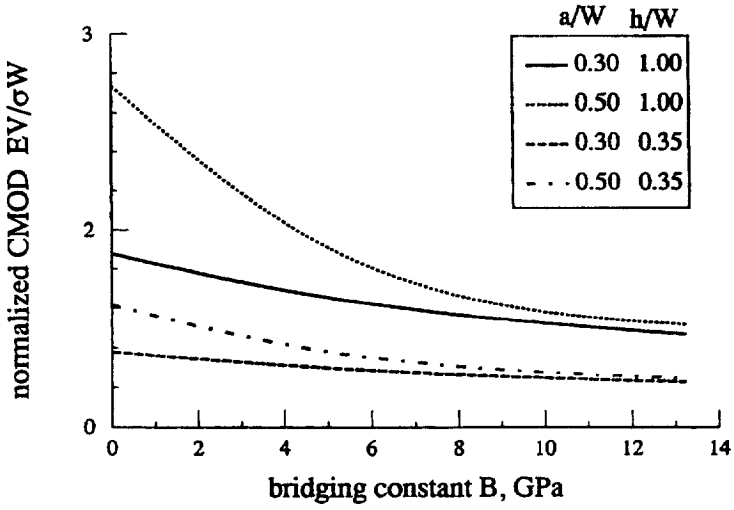


- As $\tau$ increases, the crack mouth opening displacement (CMOD) decreases

Fig. 10

# VARIATION OF THE EFFECTIVE MODULUS WITH BRIDGING CONSTANT B $\propto \sqrt{\tau}$

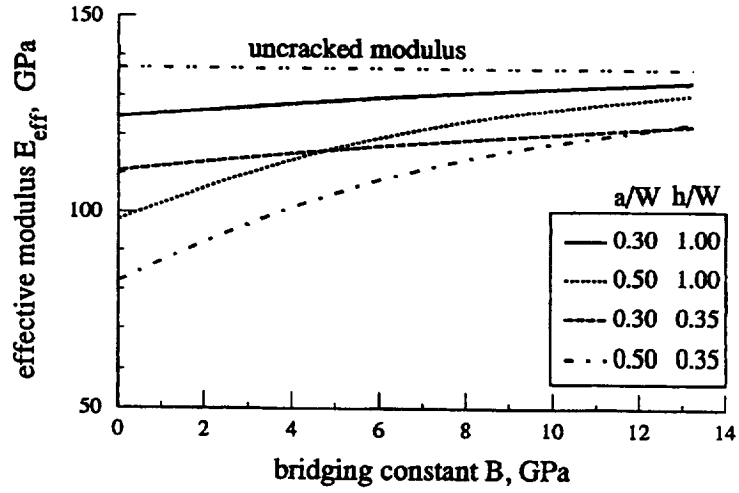


- the variation of $E_{eff}$ with crack length decreases with increasing $\tau$

Fig. 11

# BRIDGING FIBER DEGRADATION WITH TIME AT HIGH TEMPERATURE EXPOSURE

$$E_f = \frac{1}{\frac{1}{E_{f_o}} + A_o\, \sigma^{n-1}\, t^p\, e^{\left(-\frac{Q}{R\,T}\right)}}$$

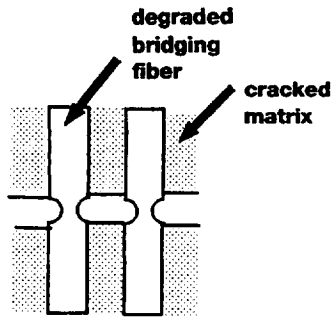


where:
- $E_f$ = effective bridging fiber modulus
- $E_{fo}$ = initial fiber modulus
- $\sigma$ = fiber closure pressure
- t = time
- T = temperature
- R = gas constant
- $A_o$, p, n, Q = empirical constant from a curve fit of fiber creep data (Ref. Morscher & DiCarlo 1991)

Fig. 12

# VARIATION OF THE STRESS INTENSITY FACTOR WITH TIME UNDER CONSTANT GLOBAL DISPLACEMENT

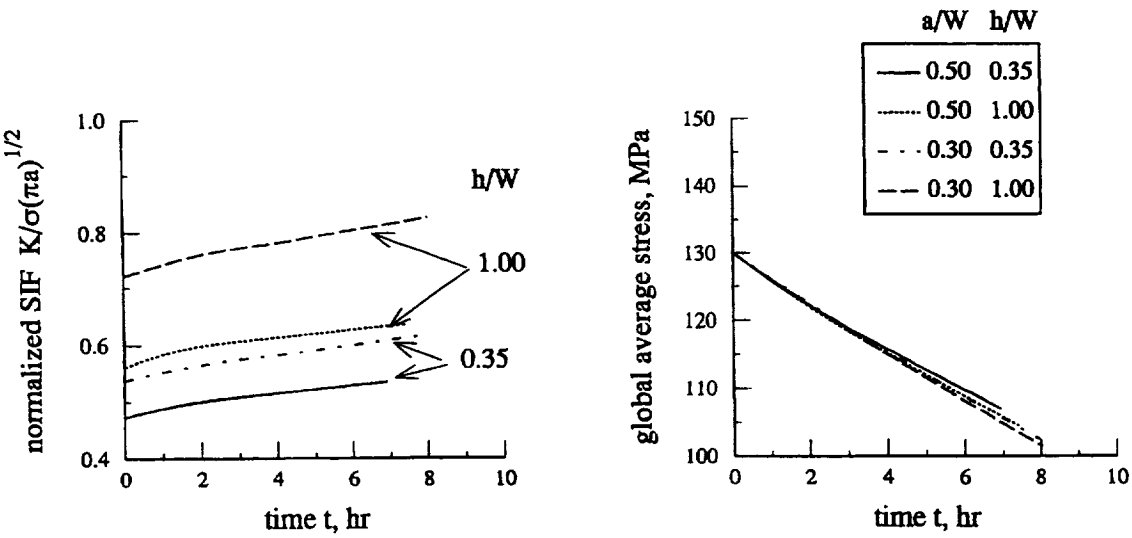


- the SIF increases with time because of the degradation of bridging fibers
- the variation of the average global stress is minimal

Fig. 13

# EFFECTS OF DISCONTINUITIES IN THE BRIDGING ZONE

**90° bundles: 0.000<a/W<0.225 & 0.450<a/W<0.675**
**0° bundles: 0.225<a/W<0.45 & 0.675<a/W<0.9**

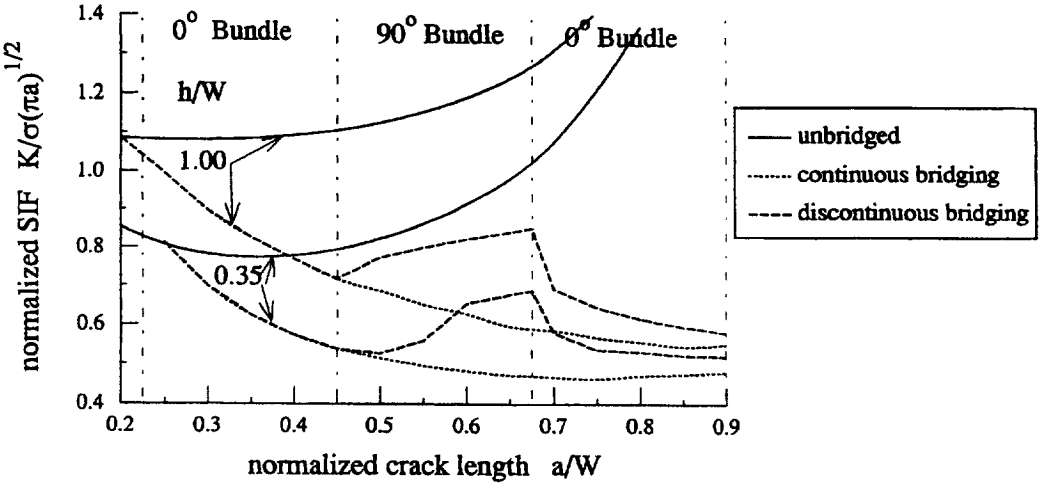


- crack growth accelerates in the 90° bundles, and decelerates in the 0° bundles

Fig. 14

# Summary

- Stress intensity factor solution in a multiple edge cracked body was established as a function of crack length and crack spacing.
- The shear lag model was used to calculate the effective stress intensity factor for multiple cracked bodies with fiber bridging.
- Variations of the effective modulus and crack opening displacement were established as a function of the crack spacing, shear lag constant, and crack length.

Fig. 15

# Conclusions

- The presence of closely spaced multiple cracks sharply reduces the stress intensity factor, and thus the crack driving forces.
- The effect of crack spacing diminishes with an increase in the interfacial frictional shear stress.
- The variation of the effective modulus and crack mouth opening displacement with crack length decreases as the bridging constant increases.

Fig. 16

# Focus of Future Research

- Calibrate the shear lag constants from experimental data.
- Incorporate the degradation of the interfacial shear stress as well as the fiber strength in the time dependent study.
- Develop a damage growth relationship based on the stress intensity factor of a bridged multiple cracked CMC component.
- Develop and verify a life prediction methodology based on the SIF for bridged multiple cracked CMCs.

Fig. 17